Received: February 8, 2024. Revised: April 15, 2024.

International Journal of
Intelligent Engineering & Systems

http://www.inass.org/

Circular Patch Antenna with Quintuple Band Operation Design Analysis and Performance Evaluation for Multi-Frequency Applications

Sahar K. Hassan[1]* Zaid M. Khudair[2]

[1]*Computer Engineering Department, College of Engineering, Al-Iraqia University, Baghdad, Iraq*
[2]*Biomedical Engineering, College of Engineering, Al-Nahrain University, Baghdad, Iraq*
sahar.k.hassan19@gmail.com

Abstract: The study presents an innovative approach to designing a Circular Microstrip Patch Antenna capable of covering a broad range of frequency bands. The physical measurements of the antenna are 34×22 × 1.57 mm³. Rogers RT5880 (Lossy) substrate has been chosen to build the antenna, which has a dielectric constant (ε_r) of 2.2. The antenna's radiating patch layer and the ground plane layer has been structured from copper, each with a thikness of 0.035 mm. The resonance at five distinct frequencies: 5.2 GHz, 6.628 GHz, 9.098 GHz, 12.036 GHz, and 13.076 GHz is the key element of this antenna. These frequencies cover a broad range of applications including WLAN, C-band, X-band, and Ku-band. Simulations has been applied using the CST Software version 2021 to validate the antenna performance. The adaptability of the antenna design, coupled with its successful validation, makes it suitable for a broad range of wireless applications across different frequency bands. This highlights their effect and applicability across a variety of technological fields.

Keywords: CST-MW, Rogers RT588 (Lossy), Micro-strip patch antenna, Multi-band.

1. Introduction

In wide range of wireless applications, the multiband microstrip patch antenna is favored by its light weighing, low cost, thin profile, and multiband operation ability. Additionally, it eliminates the need for using multiple antennas catering to different resonant frequencies [1]. An innovative method in [2, 3] presenting a novel approach featuring a proximity-linked multiband microstrip antenna that provide consistent gains and an unchanging radiation pattern. This antenna concurrently resonates within the operating frequencies of 2.4 to 2.485 GHz, 3.3 to 3.7 GHz, 5.15 to 5.35 GHz, and 5.725 to 5.85 GHz. However, these designs having a week point in the antenna's structure may introduced due to multi-layered structure and intricate geometries affecting its reliability. [4] Presents a creative concept, by using inverted L and T-shaped parasitic elements enables the designer to achieve a compact multiband mictostrip patch antenna. This design suffering from complexity of tuning. Each resonant frequency required accurate control over many parameters, which makes the design process complex and increase the probability of error during fabrication and tuning. Meanwhile, [5] employs a supplementary split-ring resonator to attain diverse multicarrier frequencies. The design involves multiple strips that need to be adjusted for each resonant frequency which is complex and require significant optimization. [6] Demonstrates a multiband consolidated inverted F antenna is operating in the Wi-Fi frequency and WiMax frequency range. The compact size and narrow bandwidth of this design may result a reduced radiation efficiency compared with larger antennas and this could impact the antenna performance. Common methodologies for achieving multiband functionality involve the utilization of U-shaped slots [7], slots incorporated into the ground layer [8], inverted F-shaped antennas [9, 10], and defected ground planes [11, 12]. However, these antenna

designs are suffering from complexity of fabrication, limited bandwidth, ground plane dependence and sensitive to manufacturing variations. Typically, these designs are tailored for operation within the 2–5 GHz frequency range, making them suitable for WiMax, Wi-Fi, GPS and Bluetooth implementations [13-15]. This article introduces a multiband circular patch antenna with the capability to resonate across five distinct frequencies, covering the WLAN, C band, X band, and Ku band frequencies (5.2 GHz, 6.6 GHz, 9 GHz, 12 GHz and 13 GHz). The proposed configuration includes an upper-side patch and a lower-side ground plane, utilizing an insert-fed approach with achieved 50Ω impedance matching between the patch and the ground plane to supply the source signal. Rogers RT5880 substrate with dimensions of 22 mm x 34 mm is placed between the upper side (Patch) and lower side (Ground plane) with dielectric constant of ε_r = 2.2 to separate the two layers. The suggested design effectively achieves return loss levels below -13 dB across all resonant frequencies allowing it to be used across wide range of wireless communications applications. The Voltage Standing Wave Ratio (VSWR) ranges between 1 and 2, providing excellent gain and directivity. Overall, the proposed multiband patch antenna presented a combination of wide frequency coverage, precise S-parameters, excellent impedance matching, and simple and optimized design, making it suitable choies for broad range of wireless communication applications.

2. The suggested microstrip antenna

The Microstrip Antenna is constructed with three tiers: Metallic elements on one face, and dielectric materials containing a ground plane layer which is located on the opposing face. While square, circular rectangular, and elliptical shapes are frequently employed patterns for microstrip patch antennas, the option exists to explore diverse uninterrupted arrangements.

2.1 The primary design of the suggested MPAs

The fundamental layout of the recently developed microstrip antenna showcasing a round patch, where the radius is denoted as a=9 mm, is illustrated in Figure 1. The primary design of the proposed MPA (Microstrip Patch Antenna) was developed using CST Studio Software. The primary design was formulated based on the mathematical equations provided below.

In the context of circular MPAs, the antenna radius (a) has been calculated by utilizing the resonant frequency (fr), as highlighted in reference [16, 17].

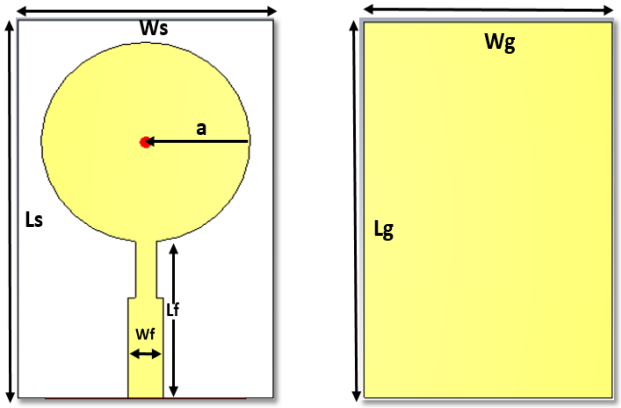

Figure. 1 Illustrates the initial attributes of the Engineered (MPAs): (a) Layout of Patches and (b) Ground Plane

$$a = \frac{8.79 \times 10^9}{f_r\sqrt{\varepsilon_r}} \quad (1)$$

The formula for calculate the antenna width (W) of the microstrip patch antenna has been derived from:

$$w_p = \frac{c}{2f_r}\sqrt{\frac{2}{\varepsilon_r + 1}} \quad (2)$$

Where: c represents the speed of light in a vacuum, fr represents the resonant frequency and ε_r stands for the effective dielectric constant of the substrate.

The formula for calculate the length (L) of a microstrip patch antenna is given by:

$$L = \frac{C}{2f_r\sqrt{\varepsilon_{eff}}} - 2\Delta L \quad (3)$$

The formula for calculate the extension length (ΔL) for a microstrip patch antenna is:

$$\Delta L = 0.412(h)\frac{(\varepsilon_{eff} + 0.3)\left(\frac{w}{h} + 0.264\right)}{(\varepsilon_{eff} - 0.258)\left(\frac{w}{h} + 0.8\right)} \quad (4)$$

The formula to calculate (ε_{eff}) for a microstrip transmission line is given by:

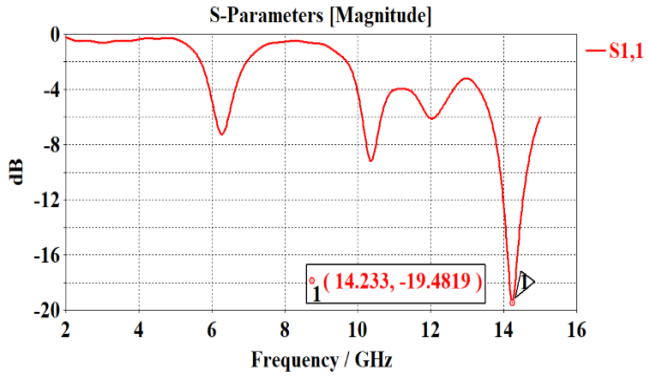

Figure. 2 S_{11} of the initial antenna

$$\varepsilon_{eff} = \frac{\varepsilon_r + 1}{2} + \frac{\varepsilon_r - 1}{2} \frac{1}{\sqrt{1 + 12\left(\frac{w}{h}\right)}} \quad (5)$$

Where: h = dielectric substrate thickness and W = microstrip line width

The antenna printed on Rogers RT5880 (Lossy) substrate, which has a dielectric constant (ε_r) of 2.2 with a thickness h=1.5 mm and area of Ws×Ls. The feed line was selected to have a length of Lf and width of Wf to allow the 50Ω impedance matching between the patch and the feed line as shown in Figure 1. The initial antenna design operates at 14.23 GHz with return loss of -19.48 dB as shown in Figure 2.

2.2 Parametric study of the proposed MPA antenna

In this section, we undertake a parametric study on the proportion of the slot in the patch antenna and investigate their effect on the antenna's performance. Figure (3) illustrate the effect of changing slot width in the patch on S_{11}, The suitable choice was setting the slot width to 5.3mm with fixed slot length of 6.9 mm.

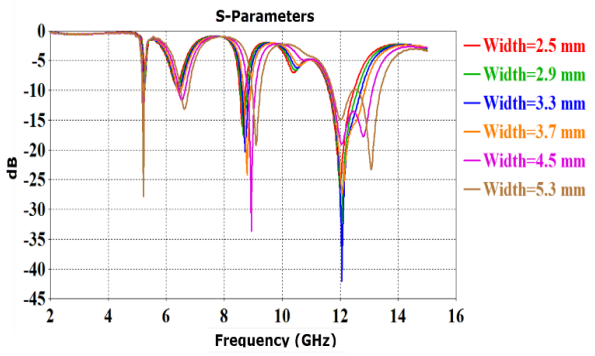

Figure. 3 illustrate the result of the impact of the slot width on S_{11} with slot length =6.9mm

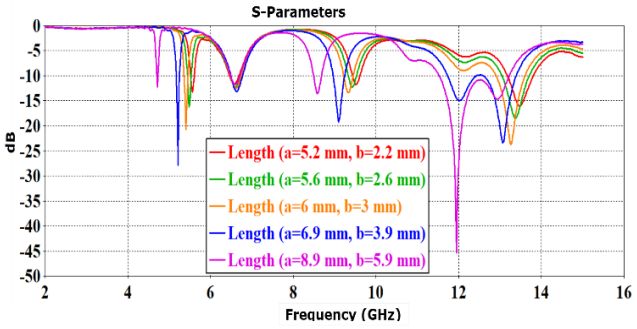

Figure. 4 illustrate the result of the effect of changing the slot length on S_{11} with fixed slot width = 5.3 mm

Figure (4) illustrate the impact of changing the slot length in the proposed patch on the return loss S_{11}, The suitable choice was setting the slot length to a = 6.9 mm and b = 3.9 mm with fixed slot width of 5.3 mm.

2.3 The final design of the proposed microstrip patch antenna

The final design for the modified circular microstrip patch antenna is shown in Figure 5.

The values of the definitive dimensions for the suggested antenna are shown in Table 1.

Figure 6 illustrates the simulated S-parameters of the antenna. Based on the final results, the S-parameters (Magnitude) has been determined to be precise. The standard value of S-parameters is set at -10 dB, which is considered as an acceptable range for wireless applications [18]. The antenna is finely adjusted to function at a frequency for optimal functionality. The simulation outcome identifies specific frequency bands: 5.2 GHz, 6.6 GHz, 9 GHz, 12 GHz, and 13 GHz. Their respective return loss values are -27.70938 dB, -13.12257 dB, -19.21219

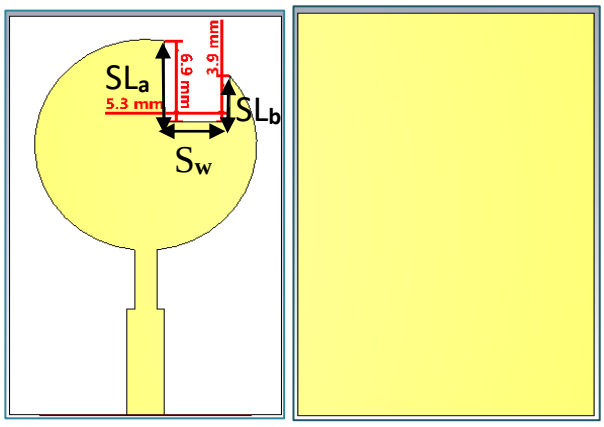

Figure. 5 The final design of Suggested Antenna: (a) Patch Structure and (b) Ground Plane

Table 1. The definitive dimensions of the suggested antenna (measured in millimeters).

Parameter	Description	Value (mm)
Ws	Total antenna width	22
Ls	Total antenna length	34
Wg	The ground width	22
Lg	The ground length	34
Wf	The feed line width	3
Sw	The slot width	5.3
SLa	The slot length a	6.9
SLb	The slot length b	3.9
Lf	The feed line length	15
t	Copper thickness	0.035
h	The substrate height	1.57
ε_r	Dielectric constant of Roggers RT5880	2.2
R	The circular patch radius	9

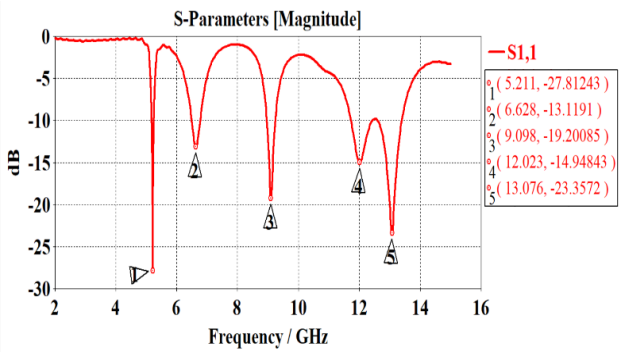

Figure. 6 Showing the Relationship between Return Loss (S_{11}) and Frequency.

dB, -14.93011 dB, and -23.35029 dB. Finally, the antenna has been designed and evaluated utilizing CST Suite Studio software.

Figure 7 illustrates the antenna gain and directivity across different frequencies. As depicted in the figure, the gain exhibits positive values at the five resonance frequencies.

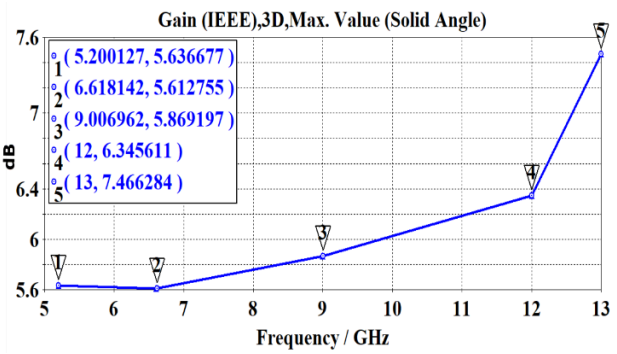

Figure. 7 Frequency-Dependent Gain Curve

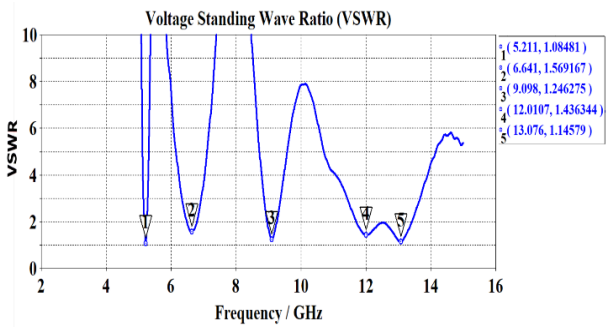

Figure. 8 Illustrates the VSWR for the suggested antennas.

Figure 8 illustrates VSWR of the antenna at its operating frequencies is close to 1. This value represents the ideal condition for achieving excellent impedance matching at the five resonant frequencies. This indicates that the reflected signals are minimal, ensuring efficient signal transmission and reception.

The diagram presented in Figure 9 (a, b) at the frequency of 5.2 GHz illustrates a directional characteristic, spanning an angle of 79.9 degrees at Phi = 90 and angle of 67.9 degree at Theta = 90. In contrast, the radiation patterns depicted in Figures 9 (c, d), 9(e, f), 9(g, h), and 9(i, j) exhibit a completely directional nature, with broader angular spans. Specifically, these patterns encompass at frequencies 6.6 GHz, 9 GHz, 12 GHz, and 13 GHz.

The radiation pattern reveals a directivity of 6.6 dBi and a main lobe direction of 1 degree at a frequency of 5.2 GHz. At a frequency of 6.6 GHz, the radiation modality demonstrates a directivity of 6.2 dBi, and the prime lobe is directed at 5 degrees. Similarly, for the 9 GHz frequency, the radiation pattern offering a directivity of 6.1 dBi, accompanied by a prime lobe direction of 1.0 degrees. Moving to the 12 GHz frequency, the radiation pattern presents a directivity of 6.7 dBi and the direction of the main lobe at 39.0 degrees. At 13 GHz, the radiation modality showcases a directivity of 7.7 dBi, and the prime lobe points at 25 degrees. These directional characteristics, along with S11 and Voltage Standing Wave Ratio (VSWR) values for several frequencies, are compiled in Table 2.

Figure 10 characterize the simulated three-dimensional radiation patterns of the suggested antenna across five operating frequencies: 5.2 GHz, 6.6 GHz, 9 GHz, 12 GHz, and 13 GHz respectively. From these patterns, it is evident that the proposed antenna exhibits a consistent unidirectional radiation pattern across all operational frequency bands. The simulated results for the distribution of surface current for the proposed microstrip antenna is

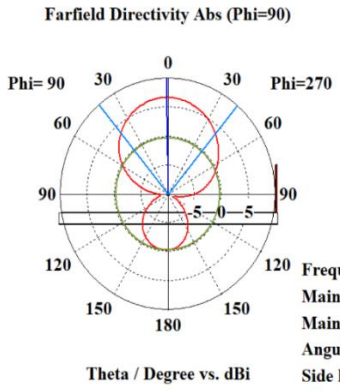

Frequency = 5.2 GHz
Main lobe magnitude = 6.64 dBi
Main lobe direction = 1.0 deg.
Angular width (3 dB) = 79.9 deg.
Side lobe level = -7.0 dB

(a)

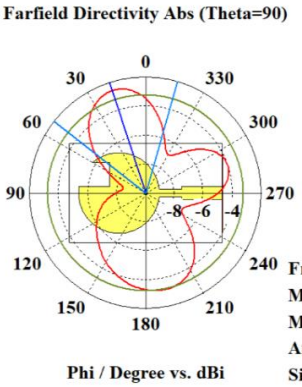

Frequency = 5.2 GHz
Main lobe magnitude = -2.59 dBi
Main lobe direction = 18.0 deg.
Angular width (3 dB) = 67.9 deg.
Side lobe level = -0.6 dB

(b)

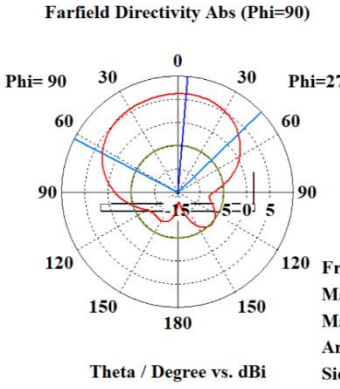

Frequency = 6.6 GHz
Main lobe magnitude = 6.17 dBi
Main lobe direction = 5.0 deg.
Angular width (3 dB) = 108.8 deg.
Side lobe level = -11.1 dB

(c)

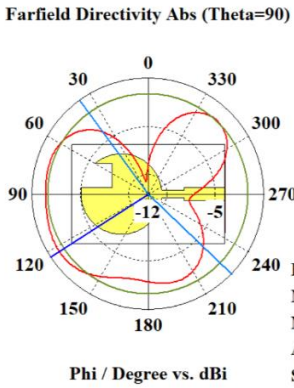

Frequency = 6.6 GHz
Main lobe magnitude = -1.08 dBi
Main lobe direction = 123.0 deg.
Angular width (3 dB) = 190.1 deg.
Side lobe level = -0.5 dB

(d)

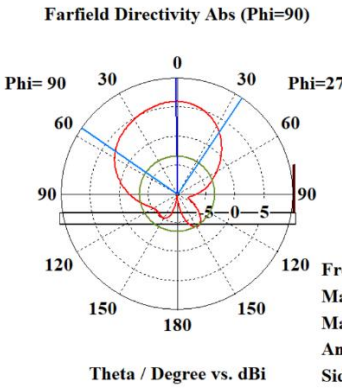

Frequency = 9 GHz
Main lobe magnitude = 5.94 dBi
Main lobe direction = 1.0 deg.
Angular width (3 dB) = 88.9 deg.
Side lobe level = -9.4 dB

(e)

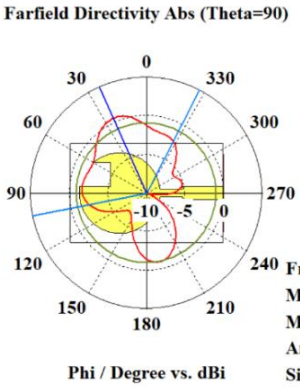

Frequency = 9 GHz
Main lobe magnitude = 0.555 dBi
Main lobe direction = 24.0 deg.
Angular width (3 dB) = 128.6 deg.
Side lobe level = -1.5 dB

(f)

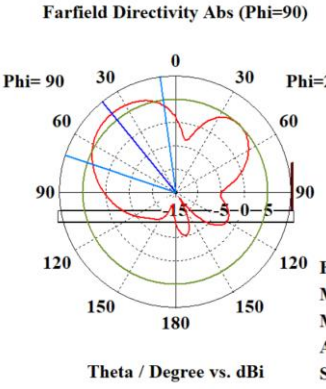

Frequency = 12 GHz
Main lobe magnitude = 6.73 dBi
Main lobe direction = 39.0 deg.
Angular width (3 dB) = 64.0 deg.
Side lobe level = -1.7 dB

(g)

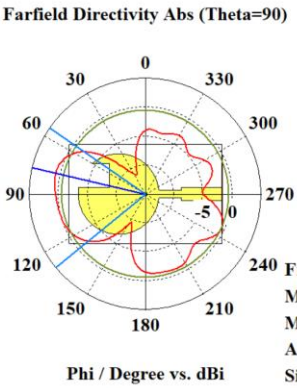

Frequency = 12 GHz
Main lobe magnitude = 0.778 dBi
Main lobe direction = 77.0 deg.
Angular width (3 dB) = 74.2 deg.
Side lobe level = -1.3 dB

(h)

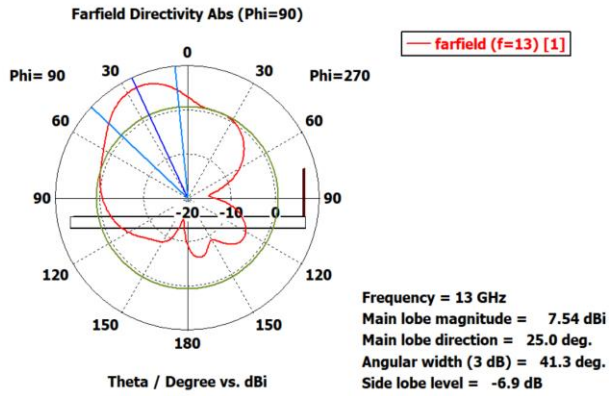

(i)

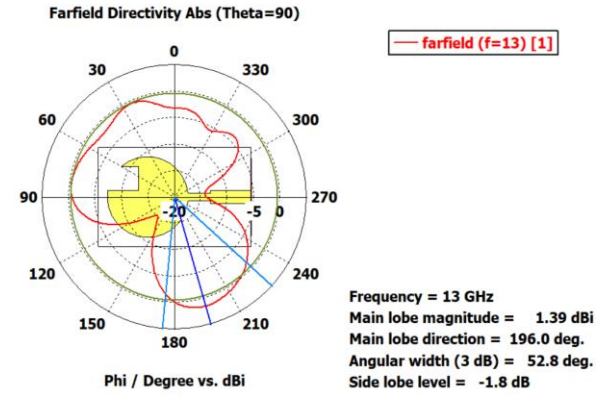

(j)

Figure. 9 The two dimensional radiation pattern of the proposed microstrip antenna: (a) 5.2GHz at Theta direction, (a) 5.2GHz at Phi direction, (c) 6.6GHz at Theta direction, (d) 6.6GHz at Phi direction, (e) 9GHz at Theta direction, (f) 9GHz at Phi direction, (g) 12 GHz at Theta direction, (h) 12 GHz at Phi direction, (i) 13GHz at Theta direction, and (j) 13GHz at Phi direction

Table 2. Reflection Loss, Voltage Standing Wave Ratio, and Directionality at Various Frequencies.

NO.	fr	S_{11}	VSWR	Directivity
1	5.2	-27.71	1.084142	6.6
2	6.6	-13.12	1.568832	6.1
3	9	-19.21	1.245914	6.1
4	12	-14.93	1.436138	6.7
5	13	-23.35	1.146049	7.7

visualized in Figure 8. At a resonant frequency of 5.2 GHz, the current exhibited a magnitude of 362 (A/m). Similarly, at 6.6 GHz, the current distribution has been observed with a magnitude of 94.6 (A/m). Notably, the current distribution demonstrated a magnitude of 152 (A/m) at 9 GHz. Furthermore, at a frequency of 12 GHz, the current distribution was measured at 99 (A/m), and 13 GHz, it was noted to be 91 (A/m).

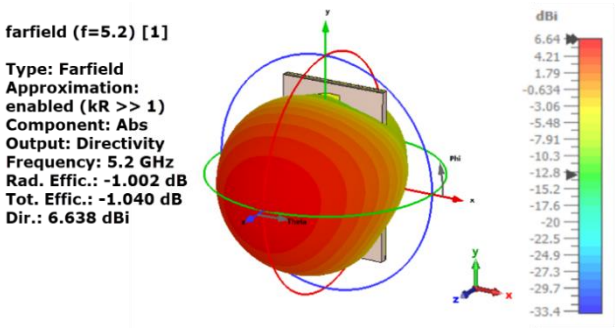

(a)

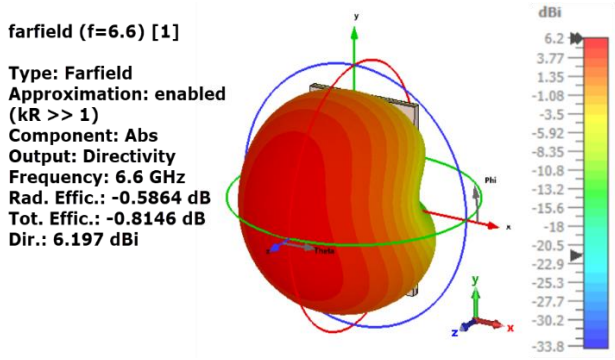

(b)

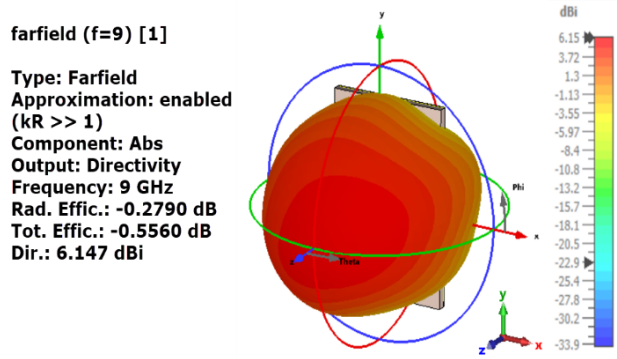

(c)

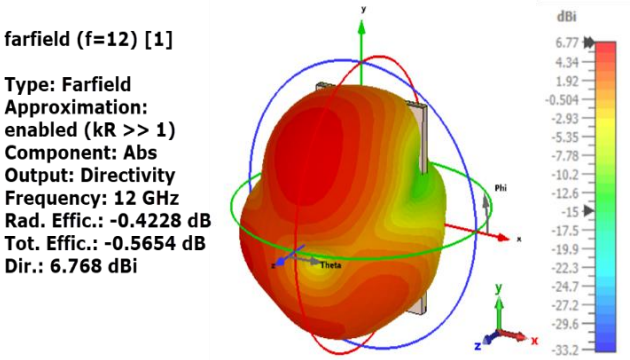

(d)

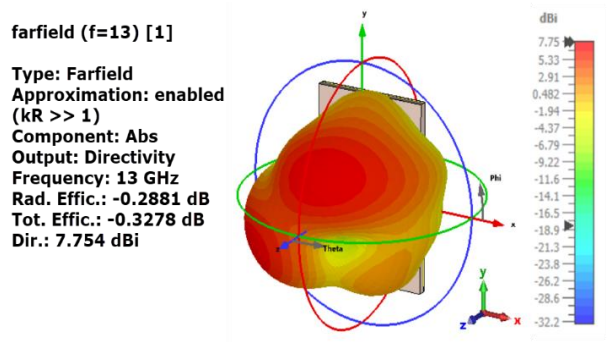

(e)

Figure. 10 Displays the simulated three dimensional radiation patterns of the suggested antenna: (a) at 5.2 GHz, (b) at 6.6 GHz, (c) at 9 GHz, (d) at 12 GHz, and (e) at 13 GHz

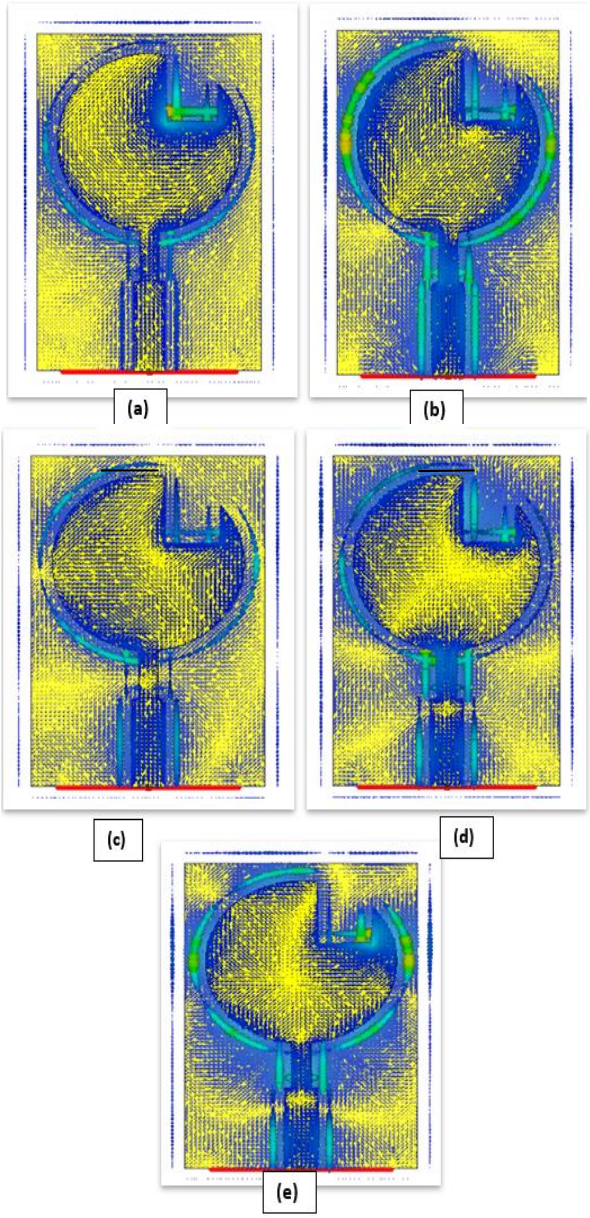

Figure. 11 Illustrates the simulated distribution of surface current for the proposed antenna: (a) at 5.2 GHz, (b) at 6.6 GHz, (c) at 9 GHz, (d) at 12 GHz, and (e) at 13 GHz

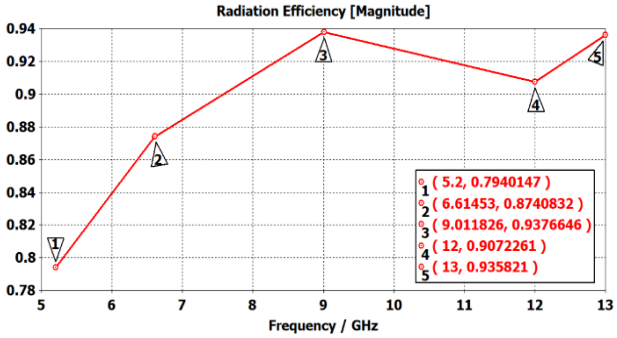

Figure. 12 Depicts the Efficiency Curve of the Proposed Antenna

(a)

(b)

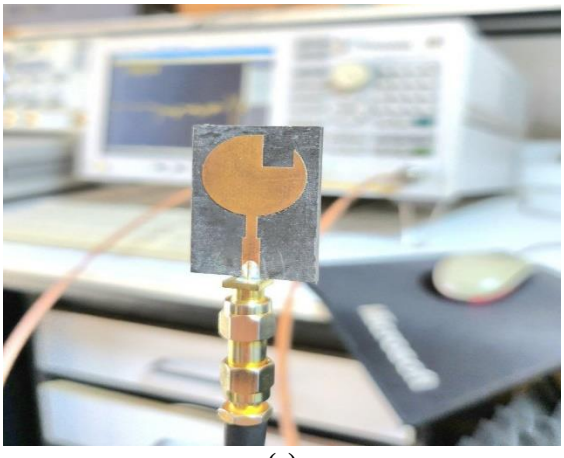

(c)

Figure. 13 The implemented Antenna: (a) Patch Layer, (b) Ground Layer, and (c) VNA measurement setup

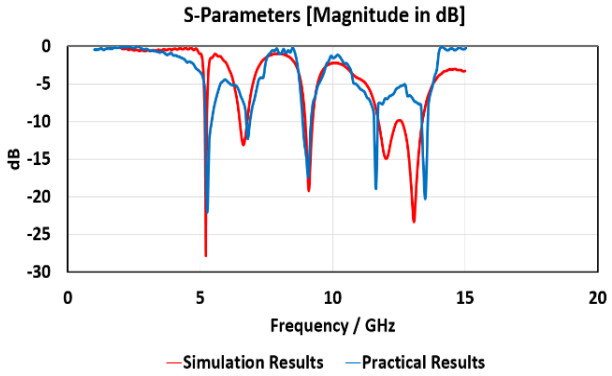

Figure. 14 Illustrate the S-Parameters (S11) of simulation and fabrication results

Figure 11 display the proposed antenna simulated surface current configuration across five operating frequencies: 5.2 GHz, 6.6 GHz, 9 GHz, 12 GHz, and 13 GHz respectively

Figure 12 illustrates the simulated radiation efficiency across the entire operating frequency range. The radiation efficiencies are measured at 79%, 87%, 94%, 91%, and 94% for the operating frequencies 5.2 GHz, 6.6 GHz, 9 GHz, 12 GHz, and 13 GHz, respectively. These values indicate that the proposed antenna is capable of efficient radiation across these frequencies.

3. Fabrication results

The suggested microstrip patch antenna has been fabricated on Rogers RT5880 substrate with dielectric constant of εr = 2.2 and a thickness of 1.57

Table 3. Presents a comparative analysis between our current research findings and prior studies

Ref.	Dimensions (mm^3)	Substrate	fr (GHz)	S_{11} (dB)	Gain (dB)
[19]	40×40	FR-4	2.42 5.33	-35.62 -28.89	3.05 2.94
[20]	35× 20	FR-4	19.14 30.02 34.91	-24.3 -18.6 -28.8	5.46 5.41 6.6
[21]	40 × 40	FR-4	3.38 5.86	-38.1 -54.9	3.05 5.78
[22]	40×30	FR-4	9.658 11.686 16.054 21.28 29.704	-33.996 -29.275 -32.855 -30.665 -32.202	6.968 2.3468 5.3692 5.8201 4.929
[23]	41 × 29	FR-4	1.7 3.6 5	−30 −24.3 −20.1	1.16-3.75
[24]	100 × 100	Rogers RT5880	1.2276 1.1765 2.492 2.3 2.5	-18.9501 -19.7478 -13.1511 -19.742 -6.8727	2.78
[25]	80 × 80	Rogers AD 255C	1.56 2.49 3.5 5.24	−15.2 −19 −22.3 −27.9	3.49–6.49
[26]	85 × 70	FR-4	1.6 2.6 3.7 5.3	−23.5 −21.5 −15.2 −22.5	3.5
The Proposed Antenna	34×22	Rogers RT5880	5.2 6.6 9 12 13	-27.71 -13.12 -19.21 -14.93 -23.35	5.6 5.6 5.9 6.3 7.5

mm as illustrated in Fig.13. The S-Parameters for the suggested antenna has been recorded using Vector Network Analyzer (VNA).

Figure 14 illustrate the difference between the simulation results and the implementation result. It is shown that practical and simulated results are reasonably accepted.

Our proposed antenna offers a distinctive advantage by covering five frequency bands simultaneously, while also achieving size reduction and gain enhancement compared to the works of other researchers. The incorporation of a single slit in the patch plane serves to amplify the gain and improve the reflection coefficient. This comprehensive approach is evident in the final patterns of gain and reflection coefficient, and their variations across the frequency spectrum.

Table 3 provides a comparative analysis between the our proposed antenna and previously reported antennas. The comparison based on dimensions, substrate type, resonance frequency, return loss and gain. The antenna in [19] was large in size and had a lower gain compared with the proposed antenna. Although the antenna in [20] had a simple design, it did not cover all the required frequencies and had lower gain compared with our design. The antenna in [21] covers only two bands and printed on Taconic RF-35 which makes its construction complicated. [22] And [23] proposed a larger antenna size compared to our antenna design with varying gain levels. In [24], [25] and [26] the designed antennas offered lower gain, limited frequency coverage and larger size compared to our proposed antenna. The comparison indicate that our proposed antenna had better characteristics compared to the previously reported antennas in term of frequency coverage, size and gain.

4. Conclusions

This research presents the design of a multiband microstrip patch antenna intended to operate within the frequency span from 2 GHz to 14 GHz. The reflection loss at all resonant frequencies. is below -13 dB, and the suggested configuration exhibits directional radiation patterns. The gain obtained is more than 7 dB. The simulation results of the suggested antenna demonstrate its favourable performance for applications in the WLAN, C band, X band, and Ku bands.

Conflicts of Interest

The authors declare no conflict of interest.

Author Contributions

Conceptualization, Sahar K. Hassan and Zaid M. Khudair; methodology, Sahar K. Hassan and Zaid M. Khudair; software, Sahar K. Hassan and Zaid M. Khudair; validation, Sahar K. Hassan and Zaid M. Khudair; formal analysis, Sahar K. Hassan; investigation, Sahar K. Hassan and Zaid M. Khudair; resources, Sahar K. Hassan and Zaid M. Khudair; data curation, Zaid M. Khudair; writing—original draft preparation, Sahar K. Hassan and Zaid M. Khudair; writing—review and editing, Sahar K. Hassan and Zaid M. Khudair; visualization, Sahar K. Hassan and Zaid M. Khudair; supervision, Sahar K. Hassan and Zaid M. Khudair; project administration, Sahar K. Hassan; funding acquisition, Sahar K. Hassan and Zaid M. Khudair.

References

[1] K. He, S. Gong, and F. Gao, “Low-profile wideband unidirectional patch antenna with improved feed structure”, *Electron. Lett*., Vol. 51, No. 4, 317–319 ,2015.

[2] P.S. Bakariya, S. Dwari, M. Sarkar, and M. K. Mandal, “Proximity-Coupled microstrip antenna for bluetooth, WiMAX, and WLAN applications”, *IEEE Antennas Wirel. Propag. Lett*., Vol. 14, 2015.

[3] Rana, Md. Sohel, and Md. Mostafizur Rahman, “Study of Microstrip Patch Antenna for Wireless Communication System”, In: *Proc. of 2022 International Conference for Advancement in Technology (ICONAT)*, 2022.

[4] J.W. Kim, T.H. Jung, H.K. Ryu, J.M. Woo, C.S. Eun, and D.K. Lee, “Compact multiband microstrip antenna using inverted-L- and T-Shaped parasitic elements”, *IEEE Antennas Wirel. Propag. Lett*., Vol. 12, 2013.

[5] J.-Y. Jan and L.-C. Tseng, “Small planar monopole antenna with a shorted parasitic inverted-L wire for wireless communications in the 2.4–5.2-, and 5.8-GHz bands”, *IEEE Trans. Antennas Propag*., Vol. 52, No. 7, pp. 1903–1905 ,2004.

[6] L. Pazin and Y. Leviatan, “Narrow-size multiband inverted-F antenna”, *IEEE Antennas Wireless Propag. Lett*., Vol. 10, pp. 139–141 ,2011.

[7] S. Shen and L. Gong, “Investigation of gain effect of multi-band patch antenna based on

composite rectangular SRRs", *Optik*, Vol. 125, pp. 930–933, 2014.

[8] A.R. Razali and M.E. Bialkowski, "Coplanar inverted-F antenna with open-end ground slots for multiband operation", *IEEE Antennas Wireless Propag. Lett*., Vol. 8, pp. 1029–1032 ,2009.

[9] H.F. Abutarboush, R. Nilavalan, T. Peter, and S.W. Cheung, "Multiband inverted-F antenna with independent bands for small and slim cellular mobilehandsets", *IEEE Trans. Antennas Propag*., Vol. 59, No. 7, pp. 2636–2645, 2011.

[10] H.W. Yang, Z.K. Yang, J.X. Liua, A.P. Li, and X. You, "A novel DGS microstrip antenna simulated by FDTD", *Optik*, Vol. 124, pp. 2277–2280 ,2013.

[11] M. Salehi and A. Tavakoli, "A novel low mutual coupling microstrip antenna array design using defected ground structure", *Int. J. Electron. Comm*., Vol. 60, No. 10, 718–723 ,2006.

[12] J. Pei, A.-G. Wang, S. Gao, and W. Leng, "Miniaturized triple-band antenna with a defected ground plane for WLAN/WiMAX applications", *IEEE Antennas Wireless Propag. Lett*., Vol. 10, pp. 298–301, 2011.

[13] H. Wang and M. Zheng, "An internal triple-band WLAN antenna", *IEEE Antennas Wireless Propag. Lett*., Vol. 10, pp. 569–572, 2011.

[14] J.H. Yoon and G.S. Kil, "Compact monopole antenna with two strips and a rectangular-slit ground plane for dual-band WLAN/WiMAX applications", *Microw. Opt. Technol. Lett*., Vol. 54, No. 7, pp. 1559–1566, 2012.

[15] A. Mehdipour, A.-R. Sebak, and C.W. Trueman, "Compact microstrip-fed antenna for 2.4/5.2/5.8 GHz wireless communication systems", In: *Proc. of IEEE AP-S Int. Symp*., pp. 1–4, 2009.

[16] S. K. Hassan, A. H. Sallomi, and M. H. Wali, "Loaded notched dual compact rectangular ultra-wideband applications monopole antenna", *Telkomnika (Telecommunication Comput. Electron. Control)*, Vol. 21, No. 3, pp. 506–512, 2023, doi: 10.12928/TELKOMNIKA.v21i3.24160.

[17] R. H. Thaher and S. N. Alsaidy, "New Compact Pentagonal Microstrip Patch Antenna for Wireless Communications Applications", *American Journal of Electromagnetics and Applications*. Vol. 6, No. 3, pp. 53–64, 2015.

[18] S. K. Hassan, A. H. Sallomi, and M. H. Wali, "Design of a Dual-Band Rejection Planar Ultra-Wideband (Uwb) Antenna", *J. Eng. Sustain. Dev*., Vol. 26, No. 4, pp. 30–35, 2022, doi: 10.31272/jeasd.26.4.3.

[19] S. J. Pawar and M. P. Joshi, "Design of dual band circular Microstrip patch antenna for ISM and WLAN", In: *Proc. of 2016 International Conference on Automatic Control and Dynamic Optimization Techniques (ICACDOT)*, pp. 608-611, 2016.

[20] A. Kakkar and S. Sah, "A Multiband Circular Patch Microstrip Antenna for K and Ka Applications", *Intelligent Communication, Control and Devices*, pp. 1437-1444, 2018.

[21] S. P. Gangwar, K. Gangwar, and A. Kumar, "Dual-band modified circular slot antenna for WLAN and WIMAX applications", *Prog. Electromagn. Res. C*, Vol. 85, pp. 247–257, 2018, doi: 10.2528/PIERC18061805.

[22] R. H. Thaher and L. M. Nori, "68 GHz), (16.054 GHz), (21.28 GHz), and (29.704 GHz) Respectively. This Antenna Operates In Wireless Applications for Operation in The X-Band", *Orig. Res.*, Vol. 10, No. 3, pp. 23–30, 2022.

[23] Z. Yu, Z. Lin, G. Zhang, Y. Li, and X. Ran, "A novel Chrysanthemum-like fractal structure multi-band antenna for mobile terminals", *International Journal of RF and Microwave Computer-Aided Engineering*, Vol. 2023, Article ID 1102668, 13 pages, 2023.

[24] A. Modi, V. Sharma, and A. Rawat, "Design and Analysis of Multilayer Patch Antenna for IRNSS, GPS, Wi-Fi, Satellite, and Mobile Networks Communications", In: *Proc. of 2021 12th Int. Conf. Comput. Commun. Netw. Technol. ICCCNT 2021*, 2021, doi: 10.1109/ICCCNT51525.2021.9580090.

[25] D. H. Patel and G. D. Makwana, "Multiband Antenna for GPS, IRNSS, Sub-6 GHz 5G and WLAN Applications", *Prog. Electromagn. Res. M*, Vol. 116, No. April, pp. 53–63, 2023, doi: 10.2528/PIERM23020902.

[26] Z. Yu, Z. Lin, X. Ran, Y. Li, B. Liang, and X.

Wang, "A novel pane structure multiband microstrip antenna for 2G/ 3G/4G/5G/WLAN/navigation applications", *International Journal of Antennas and Propagation*, Vol. 2021, article 5567417, 15 pages, 2021.